

# Gadolinium in Human Glioblastoma Cells for Gadolinium Neutron Capture Therapy<sup>1</sup>

Gelsomina De Stasio,<sup>2</sup> Patrizia Casalbore, Roberto Pallini, Benjamin Gilbert, Francesca Sanità, Maria Teresa Ciotti, Giancarlo Rosi, Armando Festinesi, Luigi Maria Larocca, Alessandro Rinelli, Didier Perret, David W. Mogk, Paolo Perfetti, Minesh P. Mehta, and Delio Mercanti

Department of Physics, University of Wisconsin-Madison, and Synchrotron Radiation Center, Stoughton, Wisconsin 53589 [G. D. S., B. G.]; Istituto di Biologia Cellulare del Consiglio Nazionale delle Ricerche, I-00137 Rome, Italy [P. C.]; Istituto di Neurochirurgia, Università Cattolica del Sacro Cuore, I-00168 Rome, Italy [R. P.]; Istituto di Neurobiologia del Consiglio Nazionale delle Ricerche, 00137 Rome, Italy [F. S., M. T. C., D. M.]; Radiobiology Department, ENEA Centro Ricerche Casaccia, I-00060 Rome, Italy [G. R., A. F.]; Istituto di Anatomia Patologica, Università Cattolica del Sacro Cuore, I-00168 Rome, Italy [L. M. L., A. R.]; Institut de Chimie Minérale et Analytique, Université de Lausanne, CH-1015 Lausanne, Switzerland [D. P.]; Department of Earth Sciences, Montana State University, Bozeman, Montana 59717 [D. W. M.]; Istituto di Struttura della Materia del Consiglio Nazionale delle Ricerche, I-00133 Rome, Italy [P. P.]; and Department of Human Oncology, University of Wisconsin, Madison Wisconsin 53792 [M. P. M.]

## ABSTRACT

<sup>157</sup>Gd is a potential agent for neutron capture cancer therapy (GdNCT). We directly observed the microdistribution of Gd in cultured human glioblastoma cells exposed to Gd-diethylenetriaminepentaacetic acid (Gd-DTPA). We demonstrated, with three independent techniques, that Gd-DTPA penetrates the plasma membrane, and we observed no deleterious effect on cell survival. A systematic microchemical analysis revealed a higher Gd accumulation in cell nuclei compared with cytoplasm. This is significant for prospective GdNCT because the proximity of Gd to DNA increases the cell-killing potential of the short-range, high-energy electrons emitted during the neutron capture reaction. We also exposed Gd-containing cells to thermal neutrons and demonstrated the GdNC reaction effectiveness in inducing cell death. These results *in vitro* stimulated *in vivo* Gd-DTPA uptake studies, currently underway, in human glioblastoma patients.

## INTRODUCTION

NCT<sup>3</sup> is a noninvasive experimental therapy for malignant gliomas based on a binary approach. In the first step, the patient is injected with an NCT agent, a tumor-seeking compound containing an isotope that has a capture cross-section for thermal neutrons many times greater than other elements present in tissue. In the second step, the patient is exposed to thermal neutrons, which induce in the NCT agent a localized, biologically destructive nuclear reaction. The most commonly used NCT agent is the isotope <sup>10</sup>B, which undergoes the reaction <sup>10</sup>B(n,α)<sup>7</sup>Li. If <sup>10</sup>B is present in tissue irradiated by a neutron flux, the majority of the radiation dose results from the high linear energy transfer products of the boron neutron capture reaction. For many years, research efforts have focused on linking the <sup>10</sup>B isotope to tumor-seeking compounds to improve the therapeutic ratio. The discovery of two boronated compounds that demonstrated tumor-seeking behavior led to clinical trials of BNCT, which are currently underway in the United States, Europe, and Japan. Preliminary results from this work demonstrate that BNCT is highly cytotoxic for malignant gliomas but because of poor specificity, a high therapeutic ratio remains elusive (1–3).

Received 12/28/00; accepted 3/16/01.

The costs of publication of this article were defrayed in part by the payment of page charges. This article must therefore be hereby marked *advertisement* in accordance with 18 U.S.C. Section 1734 solely to indicate this fact.

<sup>1</sup> The spectromicroscopy experiments were performed at the Wisconsin Synchrotron Radiation Center, a facility supported by National Science Foundation under Grant DMR-00-84402.

<sup>2</sup> To whom requests for reprints should be addressed, at Department of Physics and Synchrotron Radiation Center, University of Wisconsin-Madison, 3731 Schneider Drive, Stoughton, WI 53589. E-mail: gdestasi@facstaff.wisc.edu.

<sup>3</sup> The abbreviations used are: NCT, neutron capture therapy; BNCT, boron NCT; GdNCT, gadolinium NCT; BBB, blood-brain barrier; MRI, magnetic resonance imaging; Gd-DTPA, Gd-diethylenetriaminepentaacetic acid; ICP-MS, inductively coupled plasma mass spectrometry; ToF-SIMS, time of flight-secondary ion mass spectrometry; ME-PHISTO, microscope à émission de photoélectrons par illumination synchrotronique de type onduleur.

<sup>157</sup>Gd is a possible alternative NCT isotope to <sup>10</sup>B, although GdNCT has never been tested clinically (4–7). It is potentially a good neutron capture agent for several reasons:

(a) <sup>157</sup>Gd, which is found with a natural abundance of 15.7%, is the most effective isotope in terms of neutron capture, having the largest thermal neutron cross-section of all of the stable isotopes at 254,000 barn. By comparison, <sup>10</sup>B has 3,840 barn, <sup>16</sup>O has 0.00019 barn, <sup>12</sup>C has 0.0035 barn, <sup>1</sup>H has 0.333 barn, and <sup>14</sup>N has 1.83 barn.

(b) Several Gd compounds are known to target brain gliomas, because of the BBB disruption in these tumors. They are in fact used as tumor contrast-enhancing agents for MRI, a result of the large magnetic moment of the Gd<sup>3+</sup> ion (8).

(c) Although the Gd<sup>3+</sup> ion is itself toxic, its usefulness in MRI stimulated the search for compounds, such as the Gd-DTPA complex, which are stable in the blood stream and nontoxic. The pharmacokinetics, biodistribution, and tolerance of Gd-DTPA and other Gd compounds used for MRI are well documented (9, 10).

The Gd neutron capture reaction, <sup>157</sup>Gd(n,γ)<sup>158</sup>Gd, provokes complicated nuclear decay transitions that generate prompt gamma emission up to 7.8 MeV, accompanied by the emission of internal conversion electrons, mostly Auger electrons in the energy range ≤41 keV. Gamma rays and Auger electrons have contrasting ranges and biological effects in tissue. Gamma rays travel through the whole thickness of the tissue and are weakly absorbed by both healthy and tumor tissues. Hence, these capture products would deliver dose widely, independent of the precise location of a GdNCT agent in the tumor cells.

By contrast, mass- and charge-carrying Auger electrons are highly ionizing over a short range. The longest radiation length is on the order of tens of nanometers for the most energetic electrons. Most favorably for GdNCT, Auger electrons may induce double-strand damage if Gd is in the proximity of DNA (6); therefore, the dose enhancement attributable to the electrons emitted in the GdNCT reaction is most substantial if they originate from a site within the cell nucleus, *i.e.*, if Gd accumulated intranuclearly. Studies in the literature demonstrate that GdNCT can be used to kill tumor cells (7–11) but do not differentiate between the relative efficacies of gamma rays *versus* Auger electrons (12). It is often assumed that Gd-DTPA does not penetrate the plasma membrane, but the subcellular biodistribution of Gd-DTPA has not been evaluated adequately.

The present article specifically addresses the intracellular biolocalization question. We exposed human glioblastoma cells to Gd-DTPA and then observed Gd accumulation intracellularly and intranuclearly. We used three independent techniques to verify cellular uptake. One of these (ICP-MS) is a method of bulk analysis; the other two (X-ray spectromicroscopy and ToF-SIMS) perform microchemical surface analysis. Spectromicroscopy is a well-established technique in materials science that is still rather novel for the microchemical analysis of physiological and trace elements in biospecimens. (13–16) We used

synchrotron spectromicroscopy to directly observe the intracellular distribution of Gd, via X-ray absorption spectroscopy at the Gd 3d edge. We demonstrated that Gd-DTPA penetrates both the plasma and nuclear membranes, and our results additionally show preferential accumulation in the cell nuclei. This result was confirmed by ToF-SIMS analysis. We then exposed Gd-containing cells to thermal neutrons and demonstrated the GdNC reaction effectiveness in inducing cell death.

## MATERIALS AND METHODS

**Cell Culture and Gd-DTPA Uptake.** Primary cells were derived from tissue extracted from a patient undergoing surgery for resection of a right temporal lobe tumor. The tumor was classified as glioblastoma multiforme according to the WHO criteria (17). The tissue was finely triturated and treated with a physiological trypsin solution (0.25% trypsin, 1 mM EDTA) for 20 min at 36°C to obtain a suspension of dissociated cells. The harvested cells were propagated in DMEM supplemented with 10% FBS at 36.5°C, 5% CO<sub>2</sub>, and humidified atmosphere. Cells were always replated in the same medium once they reached confluence.

The established cell line (called TB10) was immunohistochemically characterized, and the cells stained positively for glial fibrillary acidic protein. Staining of the cells for neuronal (neuron-specific enolase, synaptophysin, and S100), endothelial (factor VIII-related antigen and CD31), epithelial (epithelial membrane antigen), lymphoid/hematopoietic (CD34, CD45, and MAC387), and cytoskeletal proteins (vimentin and cytokeratin) was negative. We therefore conclude that the cells are homogeneously glial cells. At the time of exposure to Gd, the cells were in the exponential growth phase.

Starting 24 h after plating, Gd-DTPA (Schering) was added to the culture medium to obtain concentrations of 1–25 mg/ml in the culture medium, at subsequent points in time. Exposure times varied from 0 to 120 h.

The different cell cultures for spectromicroscopy, ICP-MS, neutron bombardment, and ToF-SIMS experiments were prepared as follows.

For spectromicroscopy experiments, two series of cell cultures from different passages were prepared, in which  $5 \times 10^4$  cells/cm<sup>2</sup> were plated in 35-mm plastic Petri dishes, each containing four to five gold-plated stainless steel substrates (5-mm diameter). The Gd exposure concentration was 10 mg/ml; the exposure times were 0–72 h. At the end of the exposure periods, all dishes were carefully washed three times with PBS to remove all unbound Gd-DTPA, fixed in 4% paraformaldehyde in PBS for 20 min, and then washed in Milli-Q water. The samples were then air dried at room temperature and ashed by exposure to UV light from a low-pressure mercury lamp in the presence of ozone. UV/O<sub>3</sub> ashing selectively removes carbon and nitrogen from the cells without architectural distortion, thereby preserving the microlocalization of all other elements (18, 19). In the present study, we used it to enhance the local concentration of Gd that would otherwise not be detectable with X-ray absorption spectroscopy. The cell cultures were ashed for 116 h at a distance of 5 mm from the UV lamp.

For ICP-MS experiments to test Gd uptake *versus* exposure time, five series of cell cultures from different passages were plated in 35-mm plastic Petri dishes at a density of  $5 \times 10^4$  or  $1 \times 10^5$  cells/cm<sup>2</sup> and exposed to 10 mg/ml Gd-DTPA for 0–120 h. The different cell densities were chosen to investigate the effect of confluence on Gd uptake. At the end of the Gd incubation period, the cells were carefully washed three times with PBS before adding 1 ml of 1 N HNO<sub>3</sub> to the dishes. After 60 min of digestion at room temperature in a rocking platform, cells and liquid were collected in clean plastic tubes.

For ICP-MS experiments to test Gd uptake *versus* exposure concentration, three series of cell cultures (each one in duplicate) from different passages were plated in 35-mm plastic Petri dishes at a density of  $5 \times 10^4$  cells/cm<sup>2</sup> and exposed to 1, 5, 10, or 25 mg/ml Gd-DTPA for 72 h, beginning 24 h after plating. At the end of the exposure period, the cells were washed three times in PBS and then digested in 1 ml of 1 N HNO<sub>3</sub>. The SD of the ICP-MS experiments was calculated on the six-culture series.

For ICP-MS experiments to test Gd release after Gd exposure, two series of cell cultures from different passages were plated in 35-mm plastic Petri dishes at a density of  $5 \times 10^4$  cells/cm<sup>2</sup> and exposed to 10 mg/ml Gd-DTPA for 72 h, beginning 24 h after plating. At the end of the exposure period, the media were all replaced with 2 ml of modified Puck's saline (137 mM NaCl, 5.3 mM KCl, 6.1 mM D+Glucose, 0.1 mM CaCl<sub>2</sub>, 0.6 mM MgCl<sub>2</sub>, and 10 mM HEPES, pH

7.4) and kept at room temperature for 0–8 h, prior to harvesting in 2 ml of HNO<sub>3</sub> for ICP-MS analysis. The SD of the ICP-MS experiments on the two-culture series was within 10%.

For neutron bombardment, two series of cell cultures (each one in duplicate) from different passages were plated in plastic NUNC flask (NUNCLON; 25 cm<sup>2</sup> culture area) at a density of  $1 \times 10^4$  cells/cm<sup>2</sup> and exposed to no Gd-DTPA, 1, 5, or 10 mg/ml Gd-DTPA for 72 h, beginning 24 h after plating. At the end of the exposure period, the growth media were removed, and the flasks were filled with Puck's modified saline, in which the cells remained for 2 h before neutron bombardment. The cells were then irradiated for 1 h under a thermal neutron flux of  $3 \times 10^8$  n/cm<sup>2</sup>s (nominal power, 5 kW), at the TAPIRO fast reactor of the ENEA. The fast neutron flux at the center of the irradiation chamber (20-cm side cube) was negligible, whereas the gamma average dose was 3.2 Gy/h (20).

Two h later, the cells were detached from the plates, and cell survival was measured by cell counting and by the colorimetric 3-(4,5-dimethylthiazol-2-yl)-2,5-diphenyltetrazolium bromide assay. The SD of cell counting results using the four culture series was within 10%.

**ICP-MS.** ICP-MS provides a quantitative analysis of the concentration of an element in aqueous solution and has a sensitivity of 0.02 ppb or better for Gd (21). The analyte concentration is proportional to the number of ions of a specific element that reach the mass spectrometer from the vaporized solution at 8000°C. The analysis of cell samples in solution was performed after digestion in nitric acid and sonication. A single ICP-MS measurement represents the average of seven replicates from the same liquid sample, with a very small error (<5%). The Gd concentrations that we report in Fig. 1 at each time point were averaged across five series of cultures, ensuring that the values are correctly scaled to account for cell population differences and dilutions (based on our measurement that a volume of 1 μl contains 70,000–80,000 cells). The errors on these mean values are the SDs between the five cultures at each exposure time and represent the biological variability.

**MEPHISTO Spectromicroscopy.** Microchemical analysis of the ashed cell cultures was performed with the home-built MEPHISTO X-PEEM instrument, which uses an electron optics system (SpectroMicroTech, Orlando, FL) to form a magnified image of the photoelectrons emitted by a specimen under soft X-ray illumination. The image magnification is continuously variable up to  $\times 8000$ , and the optimum lateral resolution is 20 nm (15). The image pixel intensity (corresponding to total photoelectron yield, per unit area per unit time) is recorded as a function of photon energy. Such spectra, in fact, reflect the X-ray absorption coefficient of the specimen surface and are hence referred to as X-ray absorption spectra. The position and line shape of spectral features provide element identification and chemical state information. Spectra can be acquired simultaneously from regions selected on the real time image of the sample surface, and the probed depth is on the order of 100 Å. For this work, MEPHISTO was mounted on the HERMON beamline of the University of Wisconsin-Madison Synchrotron Radiation Center.

MEPHISTO micrographs acquired at a specific photon energy were processed in Adobe Photoshop 5.0 for Macintosh to enhance the contrast and add a scale bar. Images showing the spatial distribution of Gd and calcium were obtained by digital ratio of the pixel intensity of on- absorption peak to pre-peak micrographs.

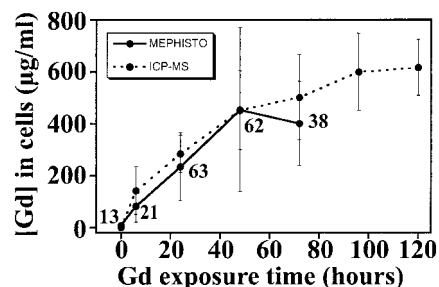


Fig. 1. The Gd uptake curve as a function of exposure time, measured by ICP-MS analysis of entire cell cultures ( $\sim 10^6$  cells) and by MEPHISTO analysis of whole-cell regions. The ICP-MS data average the results from five experimental series; bars, SD. The MEPHISTO data average the Gd signal intensities acquired on individual cells taken from two experimental series. The number of individual cells contributing to each data point is reported next to the point; bars, SD. Larger error bars, MEPHISTO data.

MEPHISTO spectra were saved as text files and plotted in Kaleidagraph 3.0.4 for Macintosh. Spectra taken from cell structures and substrate areas were normalized by dividing by a third-order polynomial fit to the raw data. Because of the weak Gd signal and high background in the X-ray absorption spectra, the systematic errors introduced by this simple normalization procedure are small compared with other experimental errors. Although in general the X-ray absorption spectra acquired in MEPHISTO may contain complicated dependencies on sample, monochromator, and beamline characteristics, the Gd 3d peaks are far from the absorption peaks of other elements, and the output of the HERMON monochromator is extremely smooth at these photon energies. Hence, spectra normalized as described produce a plot dependent only on the Gd lineshape and local concentration.

A comparison of ICP-MS and MEPHISTO data determines the calibration of MEPHISTO analysis and, therefore, quantitative information on the Gd concentration at the microscopic level. To obtain the local Gd concentration in ppm (1 ppm = 1  $\mu\text{g}/\text{ml}$ ), we multiply the Gd 3d<sub>5/2</sub> normalized peak height by 10<sup>6</sup> for unashed samples or by 10<sup>5</sup> for ashed samples, because ashing enhances the relative Gd concentration by a factor of 10. These factors were derived from the matching of MEPHISTO data from whole cells to the ICP-MS cell bulk data so that they quantitatively overlap.

This allows us to make comparisons of local Gd concentrations between different cells or subcellular structures and verify ICP-MS average results on individual cells as reported in Fig. 1.

We acquired a total of ~300 spectra from whole cells, regions of cytoplasm, nucleus, or substrate; the acquisition time for each set of spectra was 3–6 h. For the purpose of comparison of the two sets of Gd uptake *versus* exposure time measurements, acquired in MEPHISTO and with ICP-MS, we considered the spectral data from all cell regions but not substrate regions. Note that there was no Gd signal detectable from any substrate region. Of the MEPHISTO acquisition areas, we categorized 47 as coinciding with nuclei and 80 with cytoplasm. No Gd signal was detected from the 0-h sample, either with MEPHISTO or ICP-MS analysis, and no distinction was made between nuclear and cytoplasmic regions in this sample.

**ToF-SIMS.** ToF-SIMS, another technique for microchemical analysis (22), was used to further validate data from MEPHISTO spectromicroscopy. Our cell samples were bombarded with either 15 or 25 keV Ga<sup>+</sup> ions, focused in a microscopic beam, which induced desorption of the surface atoms. The emitted ions were then accelerated and detected by a high resolution mass spectrometer. By scanning the microscopic gallium ion beam, ToF-SIMS produced images of the cell surface and distribution maps of specific element isotopes, with a spatial resolution of 1  $\mu\text{m}$ . We also acquired high resolution mass spectra from microscopic areas, selected as the region of interest in the cell images, to allow quantitative comparison of Gd concentration in subcellular regions.

## RESULTS

**Bulk Uptake Kinetics.** In Fig. 1, we report quantitative ICP-MS data acquired on five series of cell cultures, exposed to Gd-DTPA for up to 120 h. The five results at each time point were averaged to produce Fig. 1, which has been rescaled to show the cellular Gd concentrations before digestion in nitric acid for ICP-MS analysis. Fig. 1 shows that the cellular Gd concentration increases with the exposure time 0–120 h.

The solid curve of Fig. 1 shows the corresponding Gd uptake kinetics in two parallel series of cell cultures, exposed to Gd-DTPA for 0–72 h and analyzed in MEPHISTO by X-ray absorption spectroscopy of individual cells. The results closely match the curve obtained from ICP-MS; the unexposed samples showed no Gd signal, whereas at other time points, the Gd concentration increased with the exposure time.

The errors in the MEPHISTO and ICP-MS data do not have identical sources, and we make the distinction between measurement errors and biological variability. For both techniques, the error on an individual measurement (as measured by replicate measurements) is acceptably small, 5–25% for X-ray absorption measurements and <5% for ICP-MS. Note that a single ICP-MS analysis takes place on

10<sup>6</sup> cells, whereas a single MEPHISTO measurement considers a fraction of a cell. The SD error bars shown on the ICP-MS data of Fig. 1 are much larger than the single measurement uncertainty because cultures exposed with identical protocols do not give the same result. This is because of a combination of fixed errors in the experimental method and intrinsic biological variation in the system. Biological variability is the major contribution to the error bars on the ICP-MS data, and this is demonstrated by the equally substantial error bars in the MEPHISTO analysis, which directly captures the variance in Gd uptake over individual cells. Because of all of the sources of experimental uncertainty, lengthy MEPHISTO analysis was performed systematically on hundreds of cells for the results presented in this article to have statistical weight.

**Gd-DTPA Toxicity and the Effect of Cell Confluence.** We explicitly looked for two effects that may affect the Gd-DTPA uptake kinetics, compound toxicity and cell density. Three independent series of cell cultures were grown at different densities and exposed for up to 120 h. Cell counting performed at the end of the incubation time either in control or in Gd-treated cultures gave the same cell number. This demonstrated that in all our experimental conditions, the cells were viable and proliferated at the same rate. Gd-DTPA did not affect cell growth; hence, it did not show any cytotoxic or cytostatic effect. Therefore, one can infer that Gd-DTPA does not release the toxic Gd<sup>3+</sup> ion that is known to reduce cell survival.

In addition, we replated some of the cells exposed to Gd-DTPA for 120 h and found that after 1 week, they grew normally and did not appear to be morphologically different from the controls.

The ICP-MS results prove that high cell density (confluence at the end of the experiment) has no detectable effect on the quantity of Gd internalized by tumor cells. The curves of Gd concentrations *versus* time at each density (correctly scaled to number of cells) could be overlapped within the error bars of Fig. 1.

**Gd Uptake in Nucleus *versus* Cytoplasm.** The agreement between ICP-MS and MEPHISTO Gd uptake curves established that X-ray absorption spectroscopy can be used to measure relative Gd concentration. The spectra were then sorted into two groups, those from cell nuclei and those from cytoplasm. In the cell cultures studied, the position of the nucleus within a cell was usually evident from the morphology apparent in the photoelectron micrographs. This was confirmed by the acquisition of calcium distribution maps, which showed the nucleus as a calcium-deficient area within the cell. In some photoelectron micrographs, the location of the nucleus was not obvious because there was no clear (topographical) nuclear boundary. Where it was not possible to confidently identify the position of the

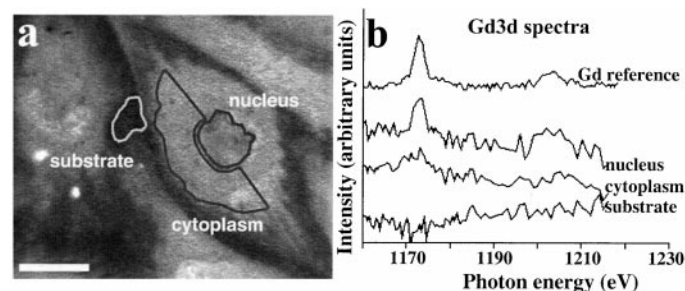


Fig. 2. *a*, calcium distribution map of a group of cells grown on a gold substrate and exposed to Gd-DTPA for 72 h. Areas containing calcium appear *bright*. Note the calcium deficiency in the nucleus and the absence of calcium between cells (*substrate* regions). Scale bar, 20  $\mu\text{m}$ . *b*, Gd 3d X-ray absorption spectra acquired simultaneously from the areas shown in *a*, plus the spectrum from a Gd-DTPA reference sample (*top curve*). No Gd was detected from the substrate region. The strongest Gd signal was obtained from the cell nucleus. This result was observed for individual cells in MEPHISTO, confirmed with independent ToF-SIMS analysis, and shown to be statistically significant by serial analysis of many cells in MEPHISTO.

Table 1 Ratio of the mean concentrations of Gd in nuclei versus cytoplasm, for each time of exposure to Gd-DTPA

The concentration on each individual cell nucleus or cytoplasm was obtained from the  $3d_{5/2}$  peak height of normalized MEPHISTO Gd spectra. The results for nuclei and cytoplasm were averaged over the number of analyzed regions reported in the table, and the ratio was calculated. At each time point, the Student *t* test was used to determine whether the increase in [Gd] in nuclei was statistically significant. At two time points, 24 and 72 h, there were significantly higher Gd concentrations in nuclei.

	Exposure time			
	6 h	24 h	48 h	72 h
[Gd] <sub>nucleus</sub> : [Gd] <sub>cytoplasm</sub> ratio	1.6	2.1	1.0	1.3
No. of data from nuclei	3	11	15	18
No. of data from cytoplasm	10	20	25	25
Student <i>t</i> test for [Gd] <sub>nucleus</sub> > [Gd] <sub>cytoplasm</sub>	Not significant	Highly significant	Not significant	Significant

Table 2 ToF-SIMS analysis of two individual ashed cells from the culture exposed to Gd-DTPA for 72 h

The local Gd concentration was measured from  $6 \times 6\text{-}\mu\text{m}^2$  areas on the nucleus or cytoplasm of each cell by recording the count rate of sputtered secondary Gd ions. The signals from all the naturally present Gd isotopes and oxides were recorded as shown and added to give the total Gd ion yield displayed in the first data column on the left. For both cells, the nucleus:cytoplasm ratio of Gd ion yield exceeded 1.5.

	Sum of isotopes	Detection rate (counts/s) for individual isotopes							
		<sup>155</sup> Gd	<sup>156</sup> Gd	<sup>158</sup> Gd	<sup>160</sup> Gd	<sup>155</sup> GdO	<sup>156</sup> GdO	<sup>158</sup> GdO	<sup>160</sup> GdO
Cell 1									
Nucleus	12.98	1.03	1.36	1.72	1.35	1.59	1.85	2.23	1.88
Cytoplasm	6.44	0.41	0.89	0.91	0.68	0.631	0.91	1.08	0.94
Ratio	2.02	2.51	1.53	1.89	1.99	2.52	2.03	2.06	2.00
Cell 2									
Nucleus	5.13	0.37	0.59	0.69	0.54	0.51	0.72	0.89	0.86
Cytoplasm	3.21	0.23	0.32	0.37	0.33	0.38	0.51	0.57	0.5
Ratio	1.60	1.60	1.84	1.86	1.63	1.34	1.41	1.56	1.72

nucleus, the spectra were excluded from analysis. An example of MEPHISTO analysis of an individual cell is presented in Fig. 2.

Fig. 2a shows a region of one of the cell culture samples (72-h exposure) imaged by MEPHISTO to show the distribution of calcium. The calcium distribution was obtained by digital ratio of a micrograph at 354 eV (on the calcium  $2p_{3/2}$  peak) to one at 352 eV (before peak) from one, and the marked cell clearly shows a central, calcium-deficient nucleus. Fig. 2b shows the corresponding Gd 3d spectra, along with a reference spectrum from Gd-DTPA. No Gd was detected from the substrate region of this or any other culture. The spectra of Fig. 2b were acquired simultaneously (except for the Gd reference) and subsequently normalized as described in "Materials and Methods."

The spectra have been displaced for clarity and contain some noise but show that the highest concentration (intensity of the Gd  $3d_{5/2}$  absorption peak at 1175 eV) of Gd is present in the cell nucleus.

A compilation of similar analyses on ~100 individual cells throughout the series of cultures showed a tendency for higher Gd concentration in nuclei than in cell cytoplasm, as shown in Table 1. This result was investigated with the Student *t* test and found to be significant or highly significant at two time points, 24 and 72 h.

The results obtained in MEPHISTO were corroborated by ToF-SIMS, an independent technique to evaluate elemental distributions at a microscopic scale. Two cells were studied from one of the ashed 72-h exposure samples used in the MEPHISTO experiment. The results obtained on these two cells are reported in Table 2. Note in Table 2 that the concentration of Gd is consistently higher in nuclei than in cytoplasm.

ToF-SIMS analysis of a non-ashed cell at the nucleus position (also Gd-exposed for 72 h) was performed before and after strong sputtering to probe the Gd concentration on the membrane and inside the nucleus. The total Gd ion yield, calculated as for the first column of Table 2, gave 0.055 counts/s on the unsputtered sample.

After 30 s sputtering (with 25 keV Ga<sup>+</sup> ions) to remove surface contamination, the total Gd ion yield from the cell membrane was 0.182 counts/s. After 16 min sputtering to penetrate ~1 μm into the nucleus, it was 1.844 counts/s. These results confirm that Gd-DTPA

had entered the cell and the nucleus and was not simply membrane bound.

**Gd Uptake versus Exposure Concentration.** To verify whether the amount of Gd internalized by the glioblastoma cells was related to the Gd concentration in the culture media, we treated the cultures with different concentrations of Gd-DTPA for the same exposure period of 72 h and analyzed them with ICP-MS. The results presented in Fig. 3 indicate that the concentration of Gd taken up increases with the exposure concentration.

Cell counting in the parallel cultures exposed to different concentrations of Gd-DTPA and unexposed controls indicated the same number of cells in each vessel, demonstrating that Gd-DTPA was not cytotoxic or cytostatic.

**Gd Release.** A significant parameter for an effective Gd-NCT is the retention time of Gd in tumor cells, after Gd washout. The results, reported in Fig. 4 indicate a substantial (~80%) and immediate loss of Gd from the cell bodies. The amount of Gd retained remains essentially constant up to 4 h and then declines again. This experiment was necessary to verify that in the neutron bombardment conditions, the cells still retained Gd.

**Neutron Irradiation.** To verify whether the 140 μg/ml of Gd retained by glioblastoma cells in the 2–4 h washout time was still

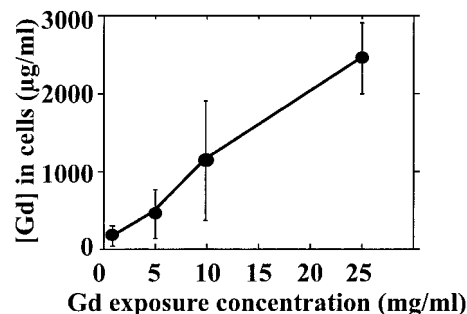


Fig. 3. Gd concentration, measured by ICP-MS, in glioblastoma cells exposed to the indicated Gd-DTPA concentrations for 72 h. Bars, SDs calculated over six cell cultures. The Gd uptake clearly increases with the Gd-DTPA exposure concentration.

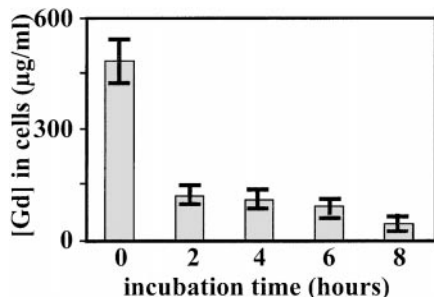


Fig. 4. Gd retention by glioblastoma cells, measured by ICP-MS, and averaged over two series of cell cultures. SD (bars) was <10%. The cell cultures were all exposed to the same Gd-DTPA concentration (10 mg/ml) for 72 h. After the incubation time, the Gd-DTPA-containing medium was removed and replaced with a physiological solution. Incubation continued for the reported periods of time at room temperature. Two to 4 h after removal of Gd-DTPA, the intracellularly retained Gd concentration was stable (140 µg/ml).

available as an efficient tumoricidal agent for NCT, we irradiated the cultures for 1 h with thermal neutrons. This experiment was performed in the absence of extracellular Gd to demonstrate that the short-range products of the Gd neutron capture reaction, *i.e.*, the Auger electrons, and not the long-range gamma rays, are responsible for double-strand DNA damage and cell death.

As shown in Fig. 5, the amount of Gd retained at the highest exposure concentrations used (10 and 5 mg/ml) was enough to produce an evident and reproducible cell death on the four cell cultures (repeated twice, each time in duplicate). The Gd concentration retained by cells exposed to 1 mg/ml Gd-DTPA, on the contrary, was not sufficient to consistently induce cell killing.

The data of Fig. 5 were obtained by direct cell count of living cells, and very similar results were obtained by the use of an 3-(4,5-dimethylthiazol-2-yl)-2,5-diphenyltetrazolium bromide assay. As presented in Fig. 5, the control cultures (no Gd) were also affected by neutron irradiation, causing 20% of the cells to die. We found that the use of the physiological solution does not impair cell viability at least for 24 h. The serum-free environment insures that the cellular mechanism of DNA repair is slowed down, resulting in principle in decreased survival of the cells in which the Gd neutron capture reaction induced DNA damage. The 20% cell killing observed in cells not exposed to Gd provides an evaluation of the extent of this phenomenon.

## DISCUSSION

The ToF-SIMS analysis of an unashed cell clearly demonstrated that Gd was internalized. Thus, the ICP-MS and MEPHISTO measurements of Gd can be confidently interpreted as measurements of the internal concentration. Cell ashing removed the carbon matrix and allowed a systematic study of intracellular localization with spectromicroscopy to provide statistical weight to the repeated observations of elevated Gd signals from nuclei relative to the surrounding cytoplasm. The MEPHISTO spectromicroscope is well suited for serial analyses of this kind (13, 19).

On a macroscopic scale, MRI routinely demonstrates that Gd compounds may be preferentially accumulated in tumor tissue *in vivo*. The degree of retention of Gd-DTPA by tumor has been correlated with the disruption of the BBB (8, 10), and this is consistent with the application of GdNCT to high-grade gliomas in which BBB disruption is severe. The present results *in vitro* prove that Gd-DTPA can penetrate the membrane of cultured cells and accumulate with an elevated concentration in cell nuclei. It has not yet been shown that this process could occur from the extracellular space of tumors in real

patients and load the cancer cells with enough  $^{157}\text{Gd}$  for NCT to be successful. The exposure times used in our experiments were long relative to the Gd-DTPA half-life in the blood ( $\sim 30$  min); therefore, multiple or continuous extended administrations need to be considered for realistic clinical cases. However, it has been estimated that a cellular concentration of 250 µg/ml is required for GdNCT to be successful (4). We achieved a maximum cellular concentration 2.4 times this value after the 120-h exposure (600 µg/ml) and >250 µg/ml after 24 h. We also found that the Gd concentration of 140 µg/ml still present in the cells after 2 h in physiological solution was sufficient to induce death in 70% of the cells with thermal neutron bombardment. These values suggest that reasonable quantities of Gd may be delivered to human tumors before the compound is removed from the blood.

Cell survival and continuous cell population increases after such long exposure times demonstrate no toxic effects of Gd-DTPA; hence, multiple administrations of the drug to a patient to maximize tumor uptake, as considered for BNCT, may be tolerated. We believe, however, that the *in vivo* situation is most clearly evaluated by directly seeking evidence of Gd-DTPA uptake by human brain tumors, and such a study is currently underway. The cell killing effect of thermal neutron irradiation further demonstrates that Gd is accumulated intracellularly and that the concentration of Gd in the cells is sufficient to induce cell death, presumably through DNA damage.

Our results are hard to compare with previous studies on the subcellular distribution and uptake of boron and Gd compounds and on their radiation effect after exposure to thermal neutrons because of the different experimental approaches. Despite these limitations, it appears that the new boronated compounds that have been developed to enhance boron uptake in cells do accumulate in human glioma cells (23–25). Boronated compounds, however, are retained in the lysosomes that are randomly distributed throughout the cytoplasm and around the cell nucleus. No selective concentration into the cell nuclei has yet been demonstrated for boronated compounds (23–25), whereas our study demonstrates that Gd preferentially concentrates in the cell nucleus. This is a strong point toward a rational design of GdNCT.

In the present study, the killing effect on cultured glioblastoma cells was  $\sim 20\%$  after radiation alone and 70% after Gd exposure followed by thermal neutrons. This finding is consistent with a cell inactivation by Gd plus thermal neutrons that is 3.5 times more effective than thermal neutrons alone. Although  $^{157}\text{Gd}$ -enriched Gd-DTPA would be preferable for GdNCT (at a greater cost), we used the naturally occurring Gd isotopic mixture. Such mixture contains 15%  $^{155}\text{Gd}$ , with a cross-section for thermal neutrons of 61,000 barn, and 15.7%  $^{157}\text{Gd}$ , with 254,000 barn; the other isotopes have <2 barn. A natural Gd mixture has a weighted, effective cross-section for thermal neu-

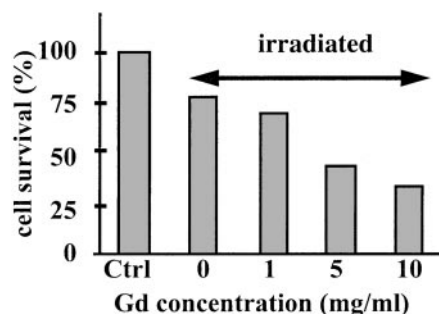


Fig. 5. Glioblastoma cell survival after neutron beam irradiation. The cell cultures were exposed to the indicated Gd-DTPA concentrations for 72 h. The Gd-DTPA media were removed and replaced with a physiological solution 2 h before the 1-h irradiation. Two h later, the cells were detached from the plates and counted. Control cultures were grown in the absence of Gd. The cell survival numbers reported were obtained averaging the results on four series of cell cultures, with SD within 10%.

trons of  $[(15 \times 61,000 + 15.7 \times 254,000)/100] = 49,028$  barn, which is still much greater than the other physiological elements present in tissue, and therefore useful for inducing selective cell killing with GdNCT.

It is reported that after irradiation with thermal neutrons, human glioma cells that have been exposed previously to boron compounds exhibit a cell inactivation that is 4.9 times more effective than neutrons alone (24). It is worth noticing that the glioma cells seem less sensitive to BNCT as compared with human colon carcinoma cells, in which boron exposure followed by thermal neutrons results to be 10.5 times more effective than the thermal neutrons alone (26).

The killing effect of BNCT also depends on the preincubation time of cells in boron-containing culture medium (27). We demonstrated that Gd reaches the highest concentration in the glioblastoma cells after 120-h exposure, and that this phenomenon is not related to a disruption of the cell membrane secondary to Gd toxicity because calcium distribution is not changed in these cells. *In vitro* and *in vivo* studies that used both malignant melanoma cells in culture and melanoma-bearing nude mice have shown a therapeutic effect at a Gd dose that is four times the accepted high dose in clinical MRI (11). Maintaining such high levels of Gd for many hours represents a practical barrier to be overcome before the development of GdNCT becomes a reality. Gd retention in glioblastoma tumor *in vivo* must be verified, and the Gd compound to use must be optimized. The present *in vitro* results, combined with *in vivo* studies, represent a safe approach to preclinical tests of Gd uptake and retention, fundamental for the optimization of GdNCT. This novel method can and will be extended to other Gd compounds [such as GdTex (28)] to select the best-suited GdNCT agent.

In conclusion, the cytotoxic products of the Gd neutron capture reaction are less clearly understood than for the boron therapy, but the much larger neutron capture cross-section of the  $^{157}\text{Gd}$  isotope makes it a promising alternative. The dose contribution of the GdNCT reaction from short-range Auger electron emission has often been neglected because it was assumed that Gd compounds remained extracellular and could not reach the cell nucleus. We show, however, that Gd-DTPA not only penetrates the plasma membrane of the cell but accumulates at higher concentration in the nucleus than in the cytoplasm.

We also prove that the nuclear Gd concentration is sufficient to induce cell killing with thermal neutron irradiation *in vitro*. These results *in vitro* stimulated *in vivo* Gd-DTPA uptake studies in human glioblastoma patients, which are currently in progress.

## ACKNOWLEDGMENTS

We thank Dr. Recep Avci of Montana State University for invaluable assistance during the ToF-SIMS experiments and Lingsu Zhang of the University of Wisconsin, Soil Science Department, for the ICM-MS analysis. We acknowledge the two unknown referees for their constructive criticism that improved the quality and the accuracy of the article.

## REFERENCES

- Haselsberger, K., Radner, H., and Pendl, G. Boron neutron capture therapy: boron distribution and pharmacokinetics of  $\text{Na}_2\text{B}_{12}\text{H}_{11}\text{SH}$  in patients with glioblastoma. *Cancer Res.*, *54*: 6318–6320, 1994.
- Smith, D. R., Chandra, S., Coderre, J. A., and Morrison, G. H. Ion microscopy imaging of  $^{10}\text{B}$  from *p*-boronophenylalanine in a brain tumor model for boron neutron capture therapy. *Cancer Res.*, *5*: 4302–4306, 1996.
- Hill, J. S., Kahl, S. B., Stylli, S. S., Nakamura, Y., Koo, M., and Kaye, A. H. Selective tumor kill of cerebral glioma by photodynamic therapy using a boronated porphyrin photosensitizer. *Proc. Natl. Acad. Sci. USA*, *92*: 12126–12130, 1995.

- Shih, J. A., and Brugger, R. M. Gadolinium as a neutron capture therapy agent. *In*: B. J. Allen, D. E. Moore, and B. V. Harrington (eds.), *Progress in Neutron Capture Therapy*, pp. 183–186. New York: Plenum Publishing Corp., 1992.
- Shih, J.-L., and Brugger, R. M. Gadolinium as a neutron capture therapy agent. *Med. Phys.*, *19*: 733–744, 1992.
- Martin, R. F., D'Chuna, G., Pardee, M., and Allen, B. J. Induction of DNA double-strand breaks by  $^{157}\text{Gd}$  neutron capture. *Pigm. Cell Res.*, *2*: 330–332, 1989.
- Laster, B. H., Shani, G., Kahl, S. B., and Warkentien, L. The biological effects of Auger electrons compared to  $\alpha$ -particles and Li ions. *Acta Oncol.*, *35*: 917–923, 1996.
- Runge, V. M., Clanton, J. A., Price, A. C., Wehr, C. J., Herzer, W. A., Partain, C. L., and James, A. E. The use of Gd-DTPA as a perfusion agent and marker of blood-brain barrier disruption. *Magn. Reson. Imaging*, *3*: 43–55, 1985.
- Weinmann, H.-J., Brasch, R. C., Press, W.-R., and Wesbey, G. E. Characteristics of gadolinium-DTPA complex: a potential NMR contrast agent. *Am. J. Roentgenol.*, *142*: 619–624, 1984.
- Yoshida, K., Furuse, M., Kaneoke, Y., Saso, K., Inao, S., Motegi, Y., Ichihara, K., and Izawa, A. Assessment of T1 time course changes and tissue-blood ratios after Gd-DTPA administration in brain tumors. *Magn. Reson. Imaging*, *7*: 9–15, 1989.
- Hofmann, B., Fischer, C.-O., Lawaczek, R., Platzek, J., and Semmler, W. Gadolinium neutron capture therapy (GdNCT) of melanoma cells and solid tumors with the magnetic resonance imaging contrast agent Gadobutrol. *Investig. Radiol.*, *34*: 126–133, 1999.
- Goorley, T., and Nikjoo, H. Electron and photon spectra for three gadolinium-based cancer therapy approaches. *Radiat. Res.*, *154*: 556–563, 2000.
- De Stasio, G., Dunham, D., Tonner, B. P., Mercanti, D., Ciotti, M. T., Angelini, A., Coluzza, C., Perfetti, P., and Margaritondo, G. Aluminum in rat cerebellar neural cultures. *Neuroreport*, *4*: 1175–1178, 1993.
- Gilbert, B., Perfetti, L., Fauchoux, O., Redondo, J., Baudat, P.-A., Andres, R., Neumann, M., Steen, S., Gabel, D., Mercanti, D., Ciotti, M. T., Perfetti, P., Margaritondo, G., and De Stasio, G. Spectromicroscopy of boron in human glioblastomas following administration of  $\text{Na}_2\text{B}_{12}\text{H}_{11}\text{SH}$ . *Phys. Rev. E*, *62*: 1110–1118, 2000.
- De Stasio, G., Perfetti, L., Gilbert, B., Fauchoux, O., Capozzi, M., Perfetti, P., Margaritondo, G., and Tonner, B. P. The MEPHISTO spectromicroscope reaches 20 nm lateral resolution. *Rev. Sci. Instrum.*, *70*: 1740–1742, 1999.
- Labrenz, M., Druschel, G. K., Thomsen-Ebert, T., Gilbert, B., Welch, S. A., Kemner, K. M., Logan, G. A., Summons, R. E., De Stasio, G., Bond, P. L., Lai, B., Kelly, S. D., and Banfield, J. F. Sphalerite (ZnS) deposits forming in natural biofilms of sulfate-reducing bacteria. *Science (Wash. DC)*, *290*: 1744–1747, 2000.
- Kleihues, P., Burger, P. C., and Scheithauer, B. W. The new WHO classification of brain tumours. *Brain Pathol.*, *3*: 255–268, 1993.
- De Stasio, G., Gilbert, B., Perfetti, L., Hansen, R., Mercanti, D., Ciotti, M. T., Andres, R., White, V. E., Perfetti, P., and Margaritondo, G. Cell ashing for trace element analysis: a new approach based on ultraviolet/ozone. *Anal. Biochem.*, *266*: 174–180, 1999.
- Gilbert, B., Perfetti, L., Hansen, R., Mercanti, D., Ciotti, M. T., Casabore, P., Andres, R., Perfetti, P., Margaritondo, G., and De Stasio, G. UV-ozone ashing of cells and tissues for spatially resolved trace element analysis. *Front. Biosci.*, *5*: 10–17, 2000.
- Pihet, P., Coppola, M., Loncol, T., Di Majo, V., and Menzel, H. G. Microdosimetry study of radiobiological facilities at the RSV-TAPIRO reactor. *Radiat. Prot. Dosim.*, *52*: 409–414, 1994.
- Frame, E. M., and Uzgiris, E. E. Gadolinium determination in tissue samples by inductively coupled plasma mass spectrometry and inductively coupled plasma atomic emission spectrometry in evaluation of the action of magnetic resonance imaging contrast agents. *Analyst*, *123*: 675–679, 1998.
- Ausserer, W. A., Ling, Y.-C., Chandra, S., and Morrison, G. H. Quantitative imaging of boron, calcium, magnesium, potassium, and sodium distributions in cultured cells with ion microscopy. *Anal. Chem.*, *61*: 2690–2695, 1989.
- Callahan, D. E., Forte, T. M., Afzal, S. M., Deen, D. F., Kahl, S. B., Bjornstad, K. A., Bauer, W. F., and Blakely, E. A. Boronated protoporphyrin (BOPP): localization in lysosomes of the human glioma cell line SF-767 with uptake modulated by lipoprotein levels. *Int. J. Radiat. Oncol. Biol. Phys.*, *45*: 3761–3771, 1999.
- Olsson, P., Black, M., Capala, J., Coderre, J., Hartman, T., Makar, M., Malmquist, J., Pettersson, J., Tilly, N., Sjöberg, S., and Carlsson, J. Uptake, toxicity, and radiation effects of the boron compounds DAAC-1 and DAC-1 in cultured human glioma cells [published erratum appears in *Int. J. Radiat. Biol.*, *73*: 452, 1998]. *Int. J. Radiat. Biol.*, *73*: 1103–1112, 1998.
- Matsumura, A., Shibata, Y., Yamamoto, T., Yoshida, F., Isobe, T., Nakai, K., Hayakawa, Y., Kiriya, M., Shimojo, N., Ono, K., Sakata, I., Nakajima, S., Okumura, M., and Nose, T. A new boronated porphyrin (STA-BX909) for neutron capture therapy: an *in vitro* survival assay and *in vivo* tissue uptake study. *Cancer Lett.*, *141*: 2203–2209, 1999.
- Tilly, N., Olsson, P., Hartman, T., Coderre, J., Makar, M., Malmquist, J., Sjöberg, S., Pettersson, J., Carlsson, J., and Glimelius, B. *In vitro* determination of toxicity, binding, retention, subcellular distribution, and biological efficacy of the boron neutron capture agent DAC-1. *Radiother. Oncol.*, *38*: 141–150, 1996.
- Ono, K., Kinashi, Y., Masunaga, S., Suzuki, M., and Takagaki, M. Effect of electrotoporation on cell killing by boron neutron capture therapy using borocaptate sodium ( $^{10}\text{B}$ -BSH). *Jpn. J. Cancer Res.*, *89*: 1352–1357, 1998.
- Bernhard, E. J., Mitchell, J. B., Deen, D., Cardell, M., Rosenthal, D. I., and Brown, J. M. Re-evaluating gadolinium(III) tetraphenyl as a radiosensitizing agent. *Cancer Res.*, *60*: 86–91, 2000.